EXPERIMENTS AND ANALYTICAL MODELING FOR DESIGNING TAPE SPRING COMPOSITES

Huina Mao[1] and Gunnar Tibert[2]

[1]PhD student, Department of Aeronautical and Vehicle Engineering, KTH Royal Institute of Technology 100 44 Stockholm, Sweden, E-mail: huina@kth.se
[2]Associate Professor, Department of Aeronautical and Vehicle Engineering, KTH Royal Institute of Technology 100 44 Stockholm, Sweden, E-mail: tibert@kth.se

Keywords: neutrally stable tape springs, bi-stable tape springs, fiber reinforced composites, viscoelasticity, tape spring design

ABSTRACT

Lightweight fiber reinforced tape spring composites are proposed for deployable space structures for nanosatellites. Neutral stable carbon fiber tape springs and bi-stable glass fiber tape springs were manufactured and their self-deployabilities after stowage were experimentally tested. The viscoelastic effects of the composites used were experimentally investigated. An analysis methodology that predicts neutral stability or bi-stability in appropriately arranging fiber directions, layups and fabric properties is presented. A design method flowchart is presented to give a reference for designing neutral or bi-stable tape springs based on the experiments and the analytical model, e.g., material type, layup, fibers direction and stability parameters. The tape spring properties before and after stowage can be predicted. The analytical model shows that fabrics of high strength fibers and low shear modulus resin with layer angle $\pm 45^\circ$ are good choices for neutrally tape springs and adding inner $0^\circ/90^\circ$ layers can increase the deployment force for bi-stable tape springs. The bi-stable glass fiber tape springs that can self-deploy after more than 6 months of stowage and high strength carbon fiber neutrally tape springs were fabricated.

1 INTRODUCTION

Tape springs are ultra-thin fiber-reinforced plastic (FRP) composites which can be folded elastically and then extended following a single kinematic path and applied to deployable booms and multi-element antennas for spacecraft [1, 2, 3]. They could be identified as unstable, bi-stable or neutrally stable by the strain energy stored in the fully coiled and fully extended configurations [4, 5]. Bi-stable tape springs are stable in both the coiled and extended states and self-deployable to construct large structures [1, 4]. Neutrally stable tape springs can be partially rolled and they neither want to unroll or rollup [3]. A proper combination of stacking sequence in the plies and prestress can achieve the unique property of neutral stability or bi-stability [3, 6]. Metallic tape springs have been widely used for space applications [7, 8]. Storable tubular extendable members (STEM) are fabricated with resilient isotropic metals and all deformations are elastic and the material is stress free in the deployed configuration. Fiber-reinforced materials have been used and are still considered for these applications because of the mass efficiency and the ability to tailor composites to exhibit behavior not seen in the traditional isotropic metals [7, 8]. A potential disadvantage of fiber-reinforced composites or tape springs is that many fiber/resin matrices exhibit time-dependent effects, e.g., viscoelastic effects. The bi-stability of the tape spring might thus be lost during stowage.

To address the nonlinear material properties and to fabricate good performance bi-stable or neutrally stable tape springs, a prediction and understanding of the properties before and after long-term stowage are vital in design. The aim of this paper is to develop an analytical design method to design tape springs that are nearly neutrally stable or bi-stable after long-term stowage.

The paper is structured as follows. In section 2, an overview of the manufactured tape springs is presented including the material properties and the stress relaxation test. In section 3, an analytical model for design of tape springs is presented. In section 4, simulation results are presented. In section 5, the design method and its applications are presented. In section 6, the conclusions of the study are presented.

2 TAPE SPRINGS AND MATERIAL PROPERTIES

Tape springs could be fabricated from dry fibers and wet prepregs with unidirectional (UD) form or fabric woven of glass, carbon, aramid and other fibers. The tape springs could be tailored based on requirements by choosing layups, thickness, material, manufacturing and etc. A woven fabric prepreg is easy to use when manufacturing tape springs.

When selecting material, the nonlinear material properties of the composites should be considered. For example, the high strain behavior of UD glass fibers laminates undergoing four point bending is nearly linear, while intermediate modulus carbon fibers exhibits significantly nonlinear behavior, [9]. The flexural stiffness of high modulus carbon fibers is initially slightly increasing, followed by a moderate reduction at 0.25% strain and finally, a sharp reduction in stiffness and failure [9]. The elastic stiffness along the glass fiber could be assumed constant, but the nonlinear properties of carbon and glass fabrics that are not in fibers direction should be studied.

To understand the behavior of different types of tape springs, nearly neutrally stable and bi-stable tape springs were manufactured, Fig. 1. A half-pipe male mode of radius 7 mm covered with release agent was used for the tape springs manufacturing. In this paper, we consider the nearly neutrally stable tape spring as being neutrally stable if the tape spring will not self-deploy from coiled state because of the static friction despite not having a flat energy surface. Two types of material were used: (i) plain weave glass fibers, Hexply M77/38%/107P/G [10], denoted M77 GF, (ii) a Twill 2X2 prepreg of high strength T300 carbon fibers, Hexply M49/42%/200T2X2/CHS-3K [11], denoted M49 CF. The plain weave and twill 2X2 fabrics are two types of woven fabrics with nearly identical fiber content in $0^\circ/90^\circ$ directions. The Instron 5567 series electric testing machine was used to get the material properties: $E_{11} = E_{22} = 63$ GPa, $G_{12} = 3.9$ GPa, $\nu_{12} = 0.23$ and $h = 0.24$ mm for M49 CF and $E_{11} = 20$ GPa, $E_{22} = 19.5$ GPa, $G_{12} = 3.5$ GPa, $\nu_{12} = 0.11$ and $h = 0.01$ mm for M77 GF, where E_{11} is the longitudinal Young's modulus, E_{22} is the transverse Young's modulus, G_{12} is the in-plane shear modulus, ν_{12} is the Poisson's ratio and h is the thickness of a single ply.

Figure 1(a) shows the carbon fiber-reinforced plastic (CFRP) tape springs made of a single ply of M49 CF cut at 45° direction, where 0° direction was oriented along the length of the tape spring. They were all bi-stable directly after manufacturing but became neutrally stable after less than half an hour of stowage with a coiled radius 10 mm at room temperature.

Figure 1(b) shows the glass fiber-reinforced plastic (GFRP) tape springs of M77 GF with three different layups, $[-45/45]$, $[-45/0/45]$ and $[45/0/90/45]$. They were all bi-stable after manufacturing and can still keep the bi-stability after more than 1 day of stowage with a coiled radius 10 mm at room temperature. Adding middle layers of $0^\circ/90^\circ$ increased the stowage ability of the bi-stable tape springs. The 4-layer, $[45/0/90/-45]$, tape spring can still self-deploy after more than 6 months of stowage.

Since the fabrics used for the manufactured tape springs, Fig. 1, contain nearly identical amount of fibers in longitude and horizontal directions, the Young's modulus E_{11}, E_{22} and Poisson's ratio ν_{12} could be assumed that they did not change with time [12]. However, the shear stiffness of the strained fabrics decreased with stowage time and was dominated by the relaxation mechanism of the epoxy resin matrix. Thus stress relaxation test is necessary to understand the decreasing shear stiffness. A constant shear strain of 1% was applied to the 4 layers, $[45]_4$, M77 GF specimen and kept for 7 days under a constant environment condition (20°C and 50% of humidity). The applied shear strain was loaded quasi-statically in 5 min to the constant one. Figure 2 shows that the shear stiffness decreased quickly in the beginning of the stress relaxation test. The initial relaxation shear stiffness, 2.3 GPa, was 34% lower than the linear

shear modulus, 3.5 GPa, because of the viscoelastic effects during the quasi-statically loading to the high shear strain, 1%. After 7 days under strain, the relaxation shear stiffness decreased to nearly 1.5 GPa, which was less than 50% of the linear shear modulus. The nonlinear shear stiffness during stowage is highly dependent on the stowage time and other factors [12, 13].

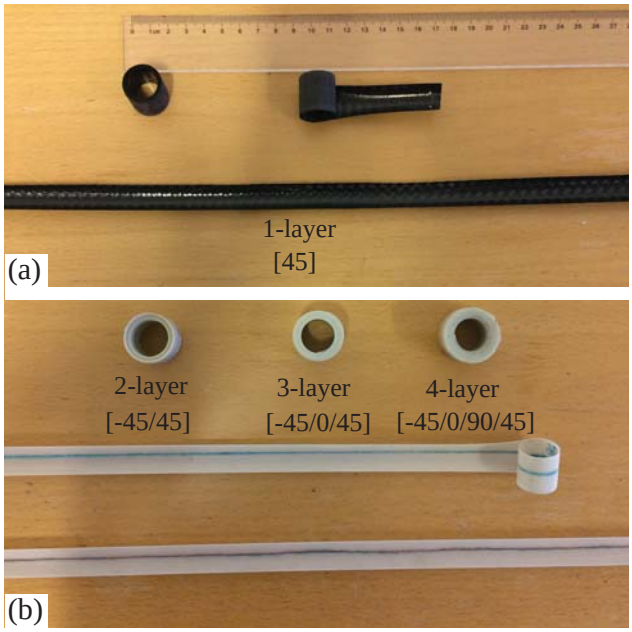

Figure 1: Tape springs: (a) carbon fiber reinforced polymer (CFRP) tape springs, and (b) glass fiber reinforced polymer (GFRP) tape springs.

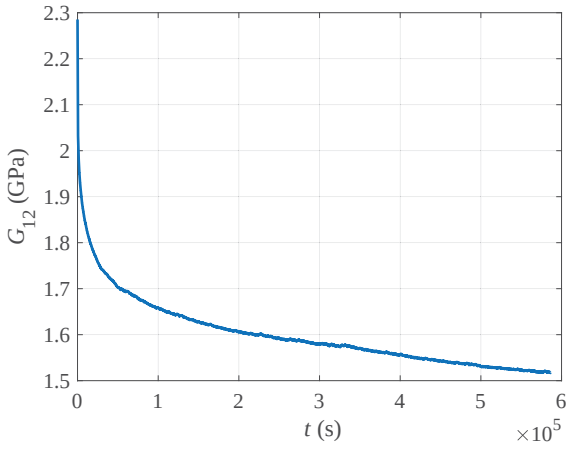

Figure 2: Stress relaxation test of M77 GF laminate: the time-dependent shear stiffness $G_{12}(t)$ decreases when subjected to a constant shear strain, $\gamma_{12} = 1\%$.

3 ANALYTICAL MODEL

In order to understand the tape spring properties before manufacturing, simple analytical models are developed in this section. Classical laminate theory is used to calculate the **ABD** matrix to connect the

applied loads, $[N_x, N_y, N_z, M_x, M_y, M_z]^T$, and associate strains, $[\varepsilon_x, \varepsilon_y, \varepsilon_z, \kappa_x, \kappa_y, \kappa_z]^T$, in the laminate [14],

$$\left[\begin{array}{c} N_x \\ N_y \\ N_z \\ \hline M_x \\ M_y \\ M_z \end{array}\right] = \left[\begin{array}{c|c} \mathbf{A} & \mathbf{B} \\ \hline \mathbf{B} & \mathbf{D} \end{array}\right] \left[\begin{array}{c} \varepsilon_x \\ \varepsilon_y \\ \varepsilon_{xy} \\ \hline \kappa_x \\ \kappa_y \\ \kappa_{xy} \end{array}\right] \tag{1}$$

where

$$A_{ij} = \sum_{k=1}^{n} \bar{Q}_{ij}(z_k - z_{k-1}) \tag{2a}$$

$$B_{ij} = \frac{1}{2}\sum_{k=1}^{n} \bar{Q}_{ij}(z_k^2 - z_{k-1}^2) \tag{2b}$$

$$D_{ij} = \frac{1}{3}\sum_{k=1}^{n} \bar{Q}_{ij}(z_k^3 - z_{k-1}^3) \tag{2c}$$

$$\bar{Q}_{11} = Q_{11}c^4 + 2(Q_{12} + 2Q_{66})c^2s^2 + Q_{22}s^4 \tag{3a}$$

$$\bar{Q}_{12} = \bar{Q}_{21} = Q_{12}(c^4 + s^4) + (Q_{11} + Q_{22} - 4Q_{66})c^2s^2 \tag{3b}$$

$$\bar{Q}_{22} = Q_{11}s^4 + 2(Q_{12} + 2Q_{66})c^2s^2 + Q_{22}c^4 \tag{3c}$$

$$\bar{Q}_{16} = \bar{Q}_{61} = (Q_{11} - Q_{12} - 2Q_{66})c^3s - (Q_{22} - Q_{12} - 2Q_{66})cs^3 \tag{3d}$$

$$\bar{Q}_{26} = \bar{Q}_{62} = (Q_{11} - Q_{12} - 2Q_{66})cs^3 - (Q_{22} - Q_{12} - 2Q_{66})c^3s \tag{3e}$$

$$\bar{Q}_{66} = (Q_{11} + Q_{22} - 2Q_{12} - 2Q_{66})c^2s^2 + Q_{66}(c^4 + s^4) \tag{3f}$$

and

$$Q_{11} = \frac{E_{11}}{1 - \nu_{12}\nu_{21}} \tag{4a}$$

$$Q_{12} = \frac{\nu_{12}E_{22}}{1 - \nu_{12}\nu_{21}} \tag{4b}$$

$$Q_{22} = \frac{E_{22}}{1 - \nu_{12}\nu_{21}} \tag{4c}$$

$$Q_{66} = G_{12} \tag{4d}$$

where z_k is the displacement of k^{th} layer to the middle layer, $c = \cos\theta$, $s = \sin\theta$, θ is the layup angle of each layer of the laminate, $\nu_{21} = \nu_{12}E_{22}/E_{11}$.

If a model is made from a symmetric layup of UD fibers, the coiled configuration would be twisted because of the coupling between bending and twisting, $D_{13} = D_{31} \neq 0$, $D_{23} = D_{32} \neq 0$. An applied bending moment will thus generate an extensional strain and undesirable static deflections and decrease the buckling load of UD fabric composites [15, 16]. Thus, the antisymmetric layup is chosen in order to achieve a compact coiled configuration [15]. However, the antisymmetric UD layup exhibits coupling between stretching and bending, matrix $\mathbf{B} \neq 0$. Woven fabrics layers can be used instead of UD fabrics to reduce the coupling problem, which creates tape springs with good strength, stiffness and superior damage tolerance over composites made from UD lamina but they may suffer from higher shear stiffness relaxation due to viscoelastic relaxation.

In this paper, woven fabrics with $E_{11} \approx E_{22}$ of each layer were used for design tape springs. Antisymmetric woven fabric layups were assumed in Section 3. Thus $D_{16} = D_{26} = 0$, $D_{11} = D_{22} > 0$, Eq. (2c). The bending moment in Eq. (1) becomes

$$\begin{bmatrix} M_x \\ M_y \end{bmatrix} = \begin{bmatrix} D_{11} & D_{12} \\ D_{12} & D_{22} \end{bmatrix} \begin{Bmatrix} \Delta\kappa_x \\ \Delta\kappa_y \end{Bmatrix} \tag{5}$$

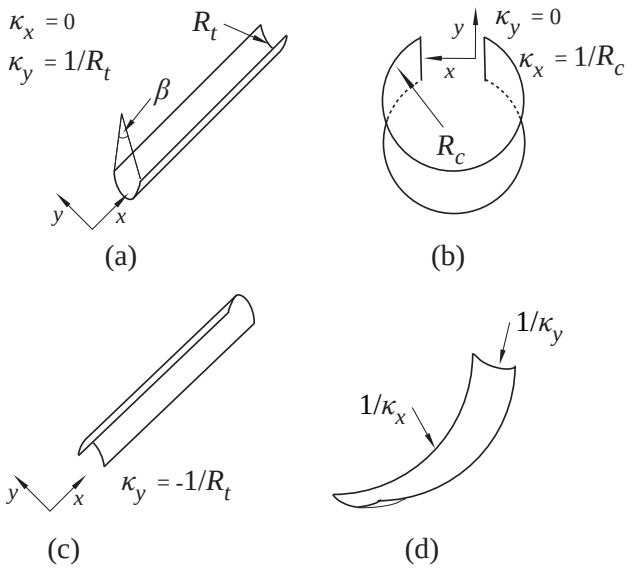

Figure 3: Tape springs configuration: (a) initial extended stable state, (b) coiled stable state, (c) opposite-sense bending stable state, (d) partially bent

Since the tape spring always has a stable equilibrium state when it is extended, Fig. 3 (a), where the curvatures $\kappa_x = 0$, $\kappa_y = 1/R_t$, and R_t is the radius of the cross section, the tape springs could be classified through the stored strain energy: (i) the tape spring is neutrally stable if the stored strain energy is the same at any position as extended state, (ii) the tape spring is bi-stable if it has another stable state at a coiled configuration but has a higher stored strain energy than that at the extended stable state. Since most of the stored strain energy of a coiled tape spring is from bending, the bending energy, U_b, could be used as the total stored strain energy [2],

$$U_b = \frac{1}{2}\Delta\kappa^T \mathbf{D} \Delta\kappa \tag{6}$$

where $\mathbf{D}$ is the bending stiffness of the tape spring in **ABD** matrix, $\Delta\kappa$ is the change of mid-surface curvatures, $\Delta\kappa = \Delta[\kappa_x, \kappa_y, \kappa_{xy}]^T$. From coiled to extend state,

$$\Delta\kappa = \begin{bmatrix} \frac{1}{R_c} \\ -\frac{1}{R_t} \\ 0 \end{bmatrix} \tag{7}$$

Then, the stored strain energy could be calculated from Eqs. (6)–(7).

3.1 Neutrally stable tape springs

If $M_x = M_y = 0$ in Eq. (5), the tape spring has the same stored strain energy as the extended state, i.e., another stable position. One solution of Eq. (5) with $M_x = M_y = 0$ is

$$\Delta\kappa_x = \sqrt{\frac{D_{22}}{D_{11}}\Delta\kappa_y^2} \tag{8}$$

where is at a stable position of the tape spring that buckled in either equal or opposite-sense bending if $D_{11} = D_{22}$, Fig. 3(b)–(c).

Another solution of Eq. (5) with $M_x = M_y = 0$ is

$$D_{11} = D_{22} = D_{12} \tag{9}$$

where the tape spring is stable at any position, Fig. 3(d), i.e., the tape spring is neutrally stable. If $D_{11} = D_{22}$ is assumed, and if

$$\frac{D_{11} - D_{12}}{D_{11}} \approx 0 \tag{10}$$

then $D_{11} = D_{22} \approx D_{12}$, where

$$D_{11} - D_{12} = \frac{1}{3}\sum_{k=1}^{n}[\bar{Q}_{11} - \bar{Q}_{12}](h_k^3 - h_{k-1}^3) \tag{11}$$

and

$$\bar{Q}_{11} - \bar{Q}_{12} = (Q_{11}c^2 - Q_{22}s^2 + Q_{12}(s^2 - c^2))(c^2 - s^2) + 8Q_{66}c^2s^2 \tag{12}$$

If the tape spring has an antisymmetric layup of $\theta = \pm 45^\circ$, Eq. (10) becomes

$$\frac{D_{11} - D_{12}}{D_{11}} = \frac{\sum_{k=1}^{n} 2Q_{66}}{\sum_{k=1}^{n}(Q_{11} + Q_{22} + 2Q_{12})/4 + Q_{66}} \tag{13}$$

If G_{12} is much smaller than E_{11} or E_{22} as for the M49 CF, Q_{66} would be much smaller than Q_{11} or Q_{22}, Eq. (3)–(4), and $D_{11} = D_{22} \approx D_{12}$, Eq. (13). Then the tape spring would be nearly neutrally stable when it has an antisymmetric layup of $\theta = \pm 45^\circ$.

If the tape spring has antisymmetric layup of $\theta = 0^\circ$, Eq. (10) becomes

$$\frac{D_{11} - D_{12}}{D_{11}} = \frac{\sum_{k=1}^{n} Q_{11} - Q_{12}}{\sum_{k=1}^{n} Q_{11}} \tag{14}$$

If the tape spring has antisymmetric layup of $\theta = 90^\circ$, Eq. (10) becomes

$$\frac{D_{11} - D_{12}}{D_{11}} = \frac{\sum_{k=1}^{n} Q_{22} - Q_{12}}{\sum_{k=1}^{n} Q_{22}} \tag{15}$$

If the fabrics have fibers at $0^\circ/90^\circ$ directions, typically $\nu_{12} < 0.5$. Then Q_{12} is much smaller than Q_{11} or Q_{22}, Eq. (3), and $(D_{11} - D_{12})/D_{11} > 0.5$. Thus adding fibers of $0^\circ/90^\circ$ to the tape spring would remove the neutral stability and turn the tape springs into a bi-stable or unstable one.

3.2 Bi-stable tape spring

If $M_x = 0$ but $M_y \neq 0$ of Eq. (5) in the coiled state, the tape spring would be bi-stable. Solving Eq. (5) of $M_x = 0$, $M_y \neq 0$, a local equilibrium position is located at,

$$\Delta\kappa_x = -\Delta\kappa_y \frac{D_{12}}{D_{11}} \tag{16}$$

where $\Delta\kappa_x = 1/R_n$, $\Delta\kappa_x = -1/R_t$ and R_n is the natural coiling radius. The local equilibrium position is the same as that presented in [15].

The bi-stability criterion for a tape spring with no coupling between bending and twisting is [15]

$$S = 4\frac{D_{66}}{D_{11}} + 2\frac{D_{12}}{D_{11}} - 2\frac{D_{22}}{D_{12}} \tag{17}$$

The structure is bi-stable or neutrally stable for $S > 0$ if the tape spring is perfectly made and no friction exists between layers. The released stored bending energy per length from a bent to fully extended configuration, calculated from Eqs. (6)–(7), is

$$F_s = U_b = \frac{\beta R_t}{2}\left[\frac{D_{11}}{R_c^2} - \frac{2D_{12}}{R_t R_c} + \frac{D_{22}}{R_t^2}\right] \tag{18}$$

Therefore if the coiled radius, R_c, and radius of the cross section, R_t, are constants, the tape spring could provide a high deployment force if fabrics have large D_{11} and D_{22} with a small D_{12}, Eq. (18). If $D_{11} = D_{22}$ as assumed, then

$$D_{11} = D_{22} = \frac{1}{3}\sum_{k=1}^{n} \bar{Q}_{11}(z_k^3 - z_{k-1}^3) = \frac{1}{3}\sum_{k=1}^{n} \left[Q_{11} - \frac{1}{2}(Q_{11} - Q_{12} - 2Q_{66})\sin^2(2\theta) \right] (z_k^3 - z_{k-1}^3) \quad (19a)$$

$$D_{12} = \frac{1}{3}\sum_{k=1}^{n} \bar{Q}_{12}(z_k^3 - z_{k-1}^3) = \frac{1}{3}\sum_{k=1}^{n} \left[Q_{12} + \frac{1}{2}(Q_{11} - Q_{12} - 2Q_{66})\sin^2(2\theta) \right] (z_k^3 - z_{k-1}^3) \quad (19b)$$

Typically $Q_{11} - Q_{12} - 2Q_{66} > 0$ because of the high tensile modulus of fibers and low shear stiffness of the matrix, Eq. (4). Therefore, if $\theta = 0^\circ$ and $\theta = 90^\circ$, D_{11} and D_{22} are maximized and D_{12} is minimized. However, if D_{12} is too small, the stability parameter would be less than zero, Eq. (17), i.e., the tape spring become unstable. Thus, antisymmetric layup fabrics that combine middle layers of $0^\circ/90^\circ$ with outer layers of other angles could generate bi-stable tape springs with high deployment force, e.g., the manufactured $[-45/0/90/45]$ GFRP tape springs.

4 SIMULATIONS

In order to predict the stability and deployability of the tape springs after manufacturing and stowage, simulations based on the analytical model in section 3 were performed and compared with the manufactured tape springs.

4.1 Neutrally stable tape spring

Section 3.1 indicates that the single-ply woven fabric having similar identity coupons fibers in both perpendicular directions could be used to make neutrally stable tape springs laid in $\pm 45^\circ$ direction. Otherwise, two layers of UD fabric with layup $[-45/45]$ could be modeled as a single-ply woven fabric.

The material properties of a tape spring can be calculated from Eqs. (1) and (20) [14].

$$E_{xx} = -\frac{A_{12}^2 - A_{11}A_{22}}{A_{22}h_t} \quad (20a)$$

$$E_{yy} = -\frac{A_{12}^2 - A_{11}A_{22}}{A_{11}h_t} \quad (20b)$$

$$G_{xy} = A_{33}/h_t \quad (20c)$$

$$\nu_{xy} = A_{12}/A_{22} \quad (20d)$$

Table 1 shows the tape springs properties made with single-ply fiber/epoxy fabric of $\theta = 45^\circ$ layup. The material properties of Kevlar, HM CF (high modulus carbon fiber) and E Glass fabrics were got from [17]. D_{12}/D_{11} is larger than 0.8 for the tape springs made of M49 CF and HM CF fabrics, and D_{12}/D_{11} is around 0.5 for tape springs of glass fabrics. Experiments show that the manufactured M49 CF fabric tape springs were not neutrally stable in the beginning, $D_{12}/D_{11} = 0.83$. However, after being coiled for half an hour, D_{12} increased as the nonlinear shear stiffness of the resin decreased, Fig. 2. For example, if G_{12} of the M49 CF fabric decreased from 3.86 GPa to 1.5 GPa after stowage, $D_{12}/D_{11} = 0.93$. The static friction between the coiled layers would likely be large enough to prevent self-deployment, i.e., it is nearly neutrally stable as observed from experiments. However, the M77 GF tape spring needed to be coiled for more than 20 days to be nearly neutrally stable. If G_{12} of the M77 GF tape spring decreased from 3.86 GPa to 1.5 GPa after one week of stowage as the stress relaxation test, Fig. 2, $D_{12}/D_{11} = 0.76$. The tape spring was still self-deployable because the stored strain energy was still large enough to counter the friction, as shown in the deployment tests. Table 1 shows that the ratio of D_{12}/D_{11} is highly dependent on the material of the reinforced fibers. A higher tensile modulus fibers provide a higher ratio of D_{12}/D_{11}, as predicted by Eq. (13), since the shear modulus of the epoxy resin matrix,

Table 1: Mechanical properties of single-ply fiber/epoxy lamina of $\theta = 45^\circ$

	M49 CF	M77 Glass	Kevlar	HM CF	E Glass
E_{xx} (GPa)	14.1	10.6	15.8	17	12.2
E_{yy} (GPa)	14.1	10.6	15.8	17	12.2
G_{xy} (GPa)	25.6	8.9	12.5	47	8.0
ν_{xy}	0.83	0.52	0.58	0.83	0.53
D_{22}/D_{11}	1	1	1	1	1
D_{12}/D_{11}	0.83	0.52	0.58	0.83	0.53

approximately to 2–5 GPa, is much smaller than the tensile modulus of the fibers. Thus the high strength carbon fibers are good choices for making nearly neutrally stable tape springs.

Table 1 shows that the ratio of D_{12}/D_{11} equals ν_{xy} of the tape spring. Thus, the Poisson's ratio of the tape spring could be used to estimate the neutrally stability of antisymmetric layup tape springs.

4.2 Bi-stable tape spring

Figure 4 shows the tape spring properties if G_{12} of the M77 GF decreased to 1.5 GPa, with two different layups, $[-\theta/0/90/\theta]$ and $[-\theta/\theta/-\theta/\theta]$. If $\theta \neq 45^\circ$, the coupling effect between bending and stretching becomes non-zero. The reduced bending stiffness $\mathbf{D}^* = \mathbf{D} - \mathbf{B}^T\mathbf{A}\mathbf{B}$ is introduced instead of the bending stiffness $\mathbf{D}$.

Figure 4(c) shows that the coupling effect between bending and stretching, B_{13}, B_{31}, B_{23}, and B_{32} increase from zero to a magnitude of 0.1 GPmm^2 as θ going away from 45°, but it is still very small. B_{11}, B_{12} and B_{21} are around zero. Analytical results shows that the properties of the tape spring is almost symmetrical to $\theta = 45^\circ$, Fig. 4. Small deviation is due to the small effect of non-zero matrix $\mathbf{B}$. The maximum stability parameter, the minimum coupling effect between bending and stretching, the minimum natural coiling radius and the minimum deployment force are all located around $\theta = 45^\circ$, as predicted in section 3.2.

Figure 4(a) shows that the tape spring is bi-stable in certain range of angles after relaxation, e.g., $36 \leq \theta \leq 54$ of layup $[-\theta/0/90/\theta]$. If the stability parameter is too high, the tape spring might become neutrally stable, i.e., cannot self-deploy due to relaxation and friction. Thus, a very small positive stability parameter is good. Sometimes, a small negative stability parameter is acceptable since the tape spring can become bi-stable due to the friction and stowage. The using of middle $0^\circ/90^\circ$ layers instead of $\theta/-\theta$ layers help the tape spring keep a small stability parameter, but it is still bi-stable in a similar range as $\theta/-\theta$; the deployment force increased 19% by using the middle layer of $0^\circ/90^\circ$ instead of $45^\circ/-45^\circ$ for the tape spring with $\pm 45^\circ$ outer layers, Fig. 4(c).

Figure 4(c) shows that the natural coiling radius increases as well when the middle $0^\circ/90^\circ$ layers are used instead of $\theta/-\theta$, Figure 4(d). The tape spring would be bi-stable if θ is between $45^\circ \pm 9^\circ$. The deployment force increases as θ goes away from 45° to $45^\circ \pm 9^\circ$. The natural coiling radius could also be used to indicate the deployment force in design when the same fabric layers of different orientations are used.

5 DESIGN METHODS AND APPLICATIONS

Figure 5 shows the design method diagram of tape springs. Once the requirements and applications of the tape springs are decided, a proper fabric material could be selected. The fabric properties and different layups are used to calculate the stability parameter, natural coiling radius, stiffness and theoretical deployment force of the tape spring. An antisymmetric layup is suggest to be used to eliminate bend-twist effects. If the plain weave has the same fiber content in both perpendicular directions ($E_{11} = E_{22}$), the antisymmetric layup becomes symmetric one. Since the small difference of fiber content in those per-

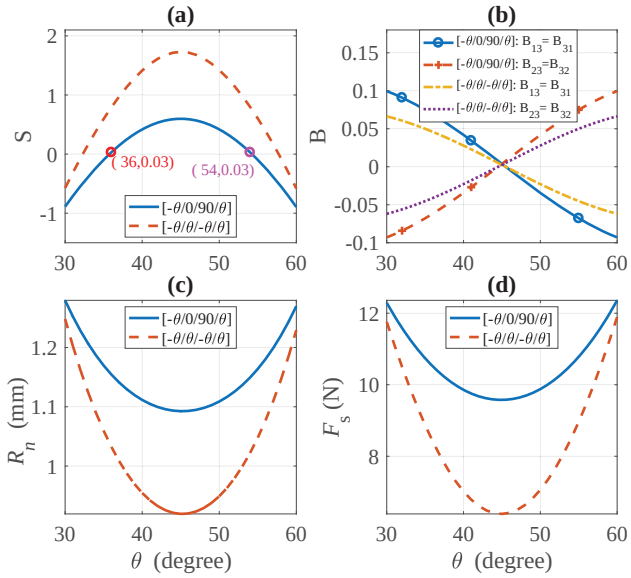

Figure 4: Tape springs property after long-term of storage, $G_{12} = 1.5$ GPa for $\pm\theta$ layers varying with ply orientation, θ, in $[-\theta/0/90/\theta]$ and $[-\theta/\theta/-\theta/\theta]$ layups: (a) stability parameters, (b) magnitude of shear strain in outsider $\pm\theta$ layers, (c) natural coiling radius, and (d) deployment force.

pendicular directions, antisymmetric layups were proposed in designs. The neutrally stable tape springs could be made by multiple antisymmetric layers of high strength woven carbon fabrics, ($E_{11} \approx E_{22}$), with lower shear modulus matrix of $\theta = \pm 45°$, e.g., $[-45/45/-45/45]$. The bi-stable tape springs could be made by antisymmetric layups of woven fabrics combined with outer layers of $\theta/-\theta$ and inner layers of $0°/90°$, e.g., $[\theta/0/90/-\theta]$. However, if $\theta \neq 45°$, very small bend-stretch effects exists. If the tape spring fulfill all the initial requirements, the nonlinear material properties of the fabrics are inserted into the design procedure to verify the tape spring properties. If all the requirements are meet, a proper tape spring is designed. Otherwise, repeat the design flow with another layup, angles, fibers thickness or material to find a proper design. If the UD fabrics are used, two layers of UD fabrics with layup $[\theta/\theta-90]$ could be modeled as a single-ply woven fabric of lay angle θ.

For example, the strain energy relaxation of transverse Young's modulus of an utrathin unidirectional carbon fiber prepreg ThinPly T800H was experimentally studied and applied to predict the deployment of long-term stowage a bi-stable tape spring in [18, 12]. However, the tape spring lost its ability to self-deploy. In order to increase the deployment force and decrease the relaxation, the design method in Fig. 5 could be used to design a good performance bi-stable tape spring. The geometrical parameters and T800H fabric elastic properties at room temperature and under relaxation tests could be find in [18]. The antisymmetric layup $[45/-45/0/45/-45]$ was used for the tape spring in the references [18, 12].

Figure 6 shows that the stability parameters and deployment force of the UD fabric tape springs are not symmetric to $\theta = 45°$ due to the UD material properties and the coupling effect between bending and stretching. The deployment force of the 5-layer tape spring, $[\theta/\theta-90/0/90-\theta/-\theta]$, could increase from 0.51 N ($\theta = 45°$) to 0.64 N ($\theta = 55°$) by adjusting the layup angles when the tape spring has no stowage, Fig. 6(a)–(b). The deployment force that after stowage could increase 60% by adjusting the angle of each layer from 0.34 N ($\theta = 45°$) to 0.55 N ($\theta = 59°$), Fig. 6(a)–(b). Since each layer is very thin ($30 \pm 1\mu m$), increasing the numbers of layers could also increase the deployment force. Figures 6(c)–(d) show that the deployment force could increase from 0.5 N to 1.6 N by adding two layers of $0°/90°$ to $[45/-45/0/45/-45]$, which gives $[45/-45/0/0/90/45/-45]$, that the deployment force increased to more than 3 times. Comparing the layup $[45/-45/0/90/45/-45]$ with $[45/-45/0/0/45/-45]$, where a $0°$ was used instead of $90°$ to the inner layer, the deployment force was almost the same, but the stability, S, decrease by using a $0°$ layer. Thus, adding a $0°$ UD layer increased stowage time and the

deployment force of the tape spring.

Manufactured tape springs show that even the theoretical stability parameter slightly smaller than 0, e.g., $S = -0.5$, the tape spring might still be bi-stable after manufacturing due to the friction between layers.

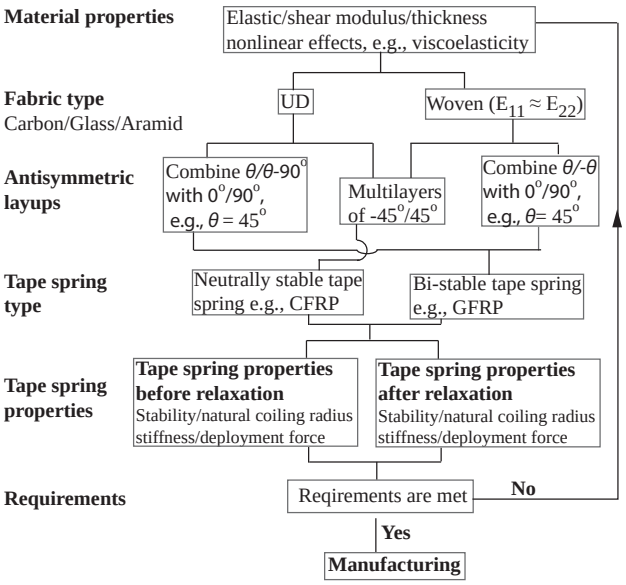

Figure 5: Flow diagram of the tape spring design model.

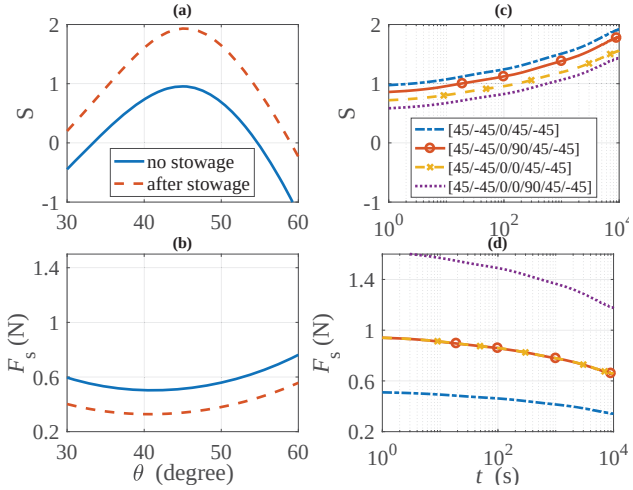

Figure 6: Stability parameter and theoretical deployment force of unidirectional carbon fiber ThinPly T800H tape spring after stowage at 60° for 3 hr: (a)–(b) 5-layers tape springs properties varying with ply orientation, θ, in $[\theta/\theta - 90/0/90 - \theta/ - \theta]$, and (c)–(d) evolution for relaxation of different layup tape springs during stowage.

6 CONCLUSIONS

The design method of making good performance neutrally stable and bi-stable tape spring are presented based on analytical models and experiments. The stress relaxation test was used to investigate the non-linear shear stiffness of FRP. The relaxation shear stiffness of the fabrics studied was dominated by the

epoxy matrix, e.g., the plain weave, twill 2X2, and UD fabric. Antisymmetric layups were suggested for tape springs to eliminate the coupling between stretching and bending.

The analytical model shows that fabrics of high strength fibers and low shear modulus resin are good choices for manufacturing neutrally tape springs of layer angle $\pm 45^\circ$. The neutrally stable tape springs were fabricated with M77 carbon fabrics; the viscoelastic effects increased the stability to be nearly neutrally stable after less than half an hour of stowage. The Poisson's ratio of the nearly neutrally stable tape spring is close to 1 after stowage.

Bi-stable tape springs that could still self-deploy after more than six months of stowage were presented. The glass fabrics of layup $[45/0/90/-45]$ were used instead of carbon fabrics to decrease the viscoelastic effects and to keep the bi-stability after long-term stowage. The analytical model, by using inner $0^\circ/90^\circ$ layers to increase the deployment force and by using $45^\circ/-45^\circ$ layers to generate bi-stability, was verified by the manufactured straight 1-meter long GFRP tape springs. The layers of $\theta \neq 45^\circ$ can increase the deployment force and decreasing the viscoelastic effects for bi-stable tape springs although a small coupling between stretching and bending exists.

The design of layups, the angle of the cross section and length of tape springs were limited by the bending stiffness and stability of the tape springs; adding more layers of the tape spring might increase the deployment force, but the tape spring might also be too stiff to be fully coiled. If using only $\pm 45^\circ$ layers for a bi-stable tape spring, it would loose too much strain energy due to relaxation. A smaller or larger angle of the cross section would make the tape spring too flexible in torsion or too wide when coiled. Thus the mechanical requirements and the tape spring properties before and after stowage should be considered during the design, Fig. 5. The design method could also be applied to design other laminates including the nonlinear material effects.

ACKNOWLEDGMENTS

I would like to thank the financial support from the European Union Seventh Framework Programme for the funding of the SEAM project. I also would like to acknowledge Anton Shipsha for the help of the experiments.

References

[1] Jeon, S. K., and Murphey, T. W., 2011. "Design and analysis of a meter-class CubeSat boom with a motor-less deployment by bi-stable tape springs". In 52nd AIAA/ASME/ASCE/AHS/ASC Structures, Structural Dynamics and Materials Conference, American Institute of Aeronautics and Astronautics.

[2] Iqbal, K., and Pellegrino, S., 2000. "Bi-stable composite shells". In 41st Structures, Structural Dynamics, and Materials Conference and Exhibit, American Institute of Aeronautics and Astronautics (AIAA).

[3] Murphey, T. W., and Pellegrino, S., 2004. "A novel actuated composite tape-spring for deployable structures". In 45th AIAA/ASME/ASCE/AHS/ASC Structures, Structural Dynamics, and Materials Conference, American Institute of Aeronautics and Astronautics.

[4] Murphey, T. W., Jeon, S., Biskner, A., and Sanford, G., 2010. "Deployable booms and antennas using bi-stable tape-springs". In 24th Annual AIAA/USU conference on small satellites. SSC10-X-6.

[5] Schultz, M. R., Hulse, M. J., Keller, P. N., and Turse, D., 2008. "Neutrally stable behavior in fiber-reinforced composite tape springs". *Composites Part A: Applied Science and Manufacturing,* **39**(6), pp. 1012–1017.

[6] Kebadze, E., Guest, S., and Pellegrino, S., 2004. "Bistable prestressed shell structures". *International Journal of Solids and Structures,* **41**(11-12), jun, pp. 2801–2820.

[7] Murphey, T. W., Francis, W. H., Davis, B. L., Mejia-Ariza, J., Santer, M., Footdale, J. N., Schmid, K., Soykasap, O., and Koorosh, G., 2015. "High strain composites". In 2nd AIAA Spacecraft Structures Conference, AIAA SciTech, American Institute of Aeronautics and Astronautics.

[8] Herlem, F., 2014. "Modelling and manufacturing of a composite bi-stable boom for small satellites". Master thesis, KTH Royal Institute of Technology, Stockholm, Sweden, June.

[9] Murphey, T. W., Peterson, M. E., and Grigoriev, M. M., 2013. "Four point bending of thin unidirectional composite laminas". In 54th AIAA/ASME/ASCE/AHS/ASC Structures, Structural Dynamics, and Materials Conference, American Institute of Aeronautics and Astronautics.

[10] Hexcel Corporation, 2014. Hexply M77 product data sheet. http://www.hexcel.com/Resources/DataSheets /Prepreg-Data-Sheets/M77_eu.pdf (Retrieved 15 March 2017).

[11] Hexcel Corporation, 2007. Hexply m49/42%/200t2×2/chs-3k, Oct. 1, 2016. http://www.lindberg-lund.com/files/Tekniske%20datablad/HEX-M49CT-TD.pdf (Retrieved 15 March 2017).

[12] Brinkmeyer, A., Pellegrino, S., and Weaver, P. M., 2015. "Effects of long-term stowage on the deployment of bistable tape springs". *Journal of Applied Mechanics,* **83**(1), nov, p. 011008.

[13] Mao, H., Ganga, P. L., Ghiozzi, M., Ivchenko, N., and Tibert, G., 2017. "Deployment of bistable self-deployable tape spring booms using a gravity offloading system". *Journal of Aerospace Engineering*, p. 04017007.

[14] Berthelot, J.-M., 1999. *Composite Materials*. Springer New York.

[15] Guest, S., and Pellegrino, S., 2006. "Analytical models for bistable cylindrical shells". *Proceedings of the Royal Society A: Mathematical, Physical and Engineering Sciences,* **462**(2067), jan, pp. 839–854.

[16] Hyer, M. W., 1981. "Some observations on the cured shape of thin unsymmetric laminates". *Journal of Composite Materials,* **15**(2), jan, pp. 175–194.

[17] Performance Composites Ltd, 2009. *Mechanical Properties of Carbon Fibre Composite Materials, Fibre/Epoxy resin (*120°*C Cure)*, July. http://www.performance-composites.com/carbonfibre/mechanicalproperties_2.asp (Retrieved 15 March 2017).

[18] Brinkmeyer, A., Pellegrino, S., and Santer, M., 2013. "Effects of viscoelasticity on the deployment of bistable tape springs". In The 19th International Conference on Composite Materials.